J. Biochem. 126, 90-97 (1999)

Roles of Asp126 and Asp156 in the Enzyme Function of Sphingomyelinase from *Bacillus cereus*[1]

Shinobu Fujii,* Kenji Ogata,* Bunpei Inoue,* Seiji Inoue,* Masahiro Murakami,† Seiji Iwama,† Shigeo Katsumura,† Masahiro Tomita,‡ Hiro-omi Tamura,§ Kikuo Tsukamoto,‖ Hiroh Ikezawa,‖ and Kiyoshi Ikeda*,[2]

**Department of Biochemistry, Osaka University of Pharmaceutical Sciences, Takatsuki, Osaka 569-1094;* †*Faculty of Science, Kwansei Gakuin University, Nishinomiya, Hyogo 662-8501;* ‡*Faculty of Engineering, Mie University, Tsu, Mie 514-8507;* §*Department of Hygienic Chemistry, Kyoritsu College of Pharmacy, Minato-ku, Tokyo 105-8512; and* ‖*Department of Microbial Chemistry, Faculty of Pharmaceutical Sciences, Nagoya City University, Nagoya, Aichi 467-8603*

Received February 24, 1999; accepted April 14, 1999

To elucidate the roles of conserved Asp residues of *Bacillus cereus* sphingomyelinase (SMase) in the kinetic and binding properties of the enzyme toward various substrates and Mg^{2+}, the kinetic data on mutant SMases (D126G and D156G) were compared with those of wild type (WT) enzyme. The stereoselectivity of the enzyme in the hydrolysis of monodispersed short-chain sphingomyelin (SM) analogs and the binding of Mg^{2+} to the enzyme were not affected by the replacement of Asp126 or Asp156. The pH-dependence curves of kinetic parameters ($1/K_m$ and k_{cat}) for D156G-catalyzed hydrolysis of micellar SM mixed with Triton X-100 (1:10) and of micellar 2-hexadecanoylamino-4-nitrophenylphosphocholine (HNP) were similar in shape to those for WT enzyme-catalyzed hydrolysis. On the other hand, the curves for D126G lacked the transition observed for D156G and WT enzymes. Comparison of the values and the shape of pH-dependence curves of kinetic parameters indicated that Asp126 of WT SMase enhances the enzyme's catalytic activity toward both substrates and its binding of HNP but not SM. The deprotonation of Asp126 enhances the substrate binding and slightly suppresses the catalytic activity toward both substrates. Asp156 of WT SMase acts to decrease the binding of both substrates and the catalytic activity to HNP but not SM. From the present study and the predicted three-dimensional structure of *B. cereus* SMase, Asp126 was thought to be located close to the active site, and its ionization was shown to affect the catalytic activity and substrate binding.

Key words: catalytic mechanism, enzyme kinetics, Mg^{2+} binding, sphingomyelinase.

Sphingomyelinases (SMases) [EC 3.1.4.12] catalyze the hydrolysis of sphingomyelin (SM) to yield ceramide and phosphocholine (*1*). SMases exist in the cells of eukaryotes such as mammals, and bacterial culture medium. In eukaryotic cells, ceramide formed through the activation of SMase may function as a second messenger in mediating cell growth, differentiation, stress responses, and apoptosis (*2, 3*).

Recently, the cloning of mouse and human neutral Mg^{2+}-dependent SMases suggested that the residues important for Mg^{2+} binding and catalytic activity in a large family of Mg^{2+}-dependent phosphodiesterases as well as bacterial SMases are all conserved in the amino acid sequences of these enzymes (*4*). This indicates that the catalytic mechanism of bacterial SMases is similar to that of mammalian enzymes.

Previously, we studied the binding of Mg^{2+} and the pH-dependence of kinetic parameters for the hydrolysis of micellar substrates catalyzed by SMase from *Bacillus cereus* (*5*). The results indicated that this enzyme possesses at least two binding sites for Mg^{2+}, and that the binding of Mg^{2+} to the low-affinity site was essential for the catalysis and was independent of the binding of substrate to the enzyme. The pH-dependence data of the kinetic parameters showed that one and three ionizable groups participated in the substrate binding and catalytic activity, respectively. On the basis of these results, we proposed a general-base catalysis as the catalytic mechanism of *B. cereus* SMase.

We performed site-directed mutagenesis in the sequence of *B. cereus* SMase (*6-8*), converting separately four Asp and two His residues in the conserved regions of bacterial SMases into Gly and Ala, respectively. The enzymatic activities of the mutants D295G, H151A, and H296A were drastically reduced, whereas that of D233G was not markedly changed. The activities of D126G and D156G

[1] A part of this work was supported by a Grant-in-Aid for the Encouragement of Young Scientists to S.F. and one for Scientific Research to K. I. from the Ministry of Education, Science, Sports and Culture of Japan.

[2] To whom correspondence should be addressed. Tel/Fax: +81-726-90-1075, E-mail: ikeda@oysun01.oups.ac.jp

Abbreviations: HNP, 2-hexadecanoylamino-4-nitrophenylphosphocholine; C_6C_{10}DSPC, *N*-hexanoyl-C_{10}-dihydrosphingosylphosphocholine; C_6C_{10}SPC, *N*-hexanoyl-C_{10}-sphingosylphosphocholine; lyso-PC, lysophosphatidylcholine; *p*-NPPC, *p*-nitrophenylphosphocholine; SM, sphingomyelin; SMase, sphingomyelinase; WT, wild type.

toward SM were reduced by more than 50%. The activity of D126G toward HNP was also reduced as compared to that of the wild type (WT) enzyme, whereas the activity of D156G toward HNP was greatly enhanced.

In the present study, in order to elucidate the roles of Asp126 and Asp156 in the enzyme function of *B. cereus* SMase, a detailed kinetic analysis of D126G and D156G SMase was carried out in comparison with the WT enzyme.

MATERIALS AND METHODS

Materials—Sphingomyelin (SM) from bovine brain, 2-hexadecanoylamino-4-nitrophenylphosphocholine (HNP), and Triton X-100 were obtained from Sigma. Extra-pure $MgCl_2 \cdot 6H_2O$ and NaCl were obtained from Wako Pure Chemicals and Matsunaga Chemicals, respectively.

Stereoisomers of short-chain SM analogs (*N*-hexanoyl-C_{10}-sphingosylphosphocholine, C_6C_{10}SPC; and *N*-hexanoyl-C_{10}-dihydrosphingosylphosphocholine, C_6C_{10}DSPC) were synthesized as previously described (*9*). Concentrations of the analogs were determined by quantitative analysis of phosphorus according to the method of Fiske and Sabbarow (*10*).

SMase from *B. cereus* was purchased from Higeta Shouyu. Expression in *Bacillus brevis* 47 and purification of mutant SMases, D126G and D156G, were carried out essentially as previously described (*6*). SMase was dissolved in 8 M urea, then dialyzed against 0.2 M NaCl, and centrifuged. The resulting supernatant was chromatographed on a Sephadex G-100 column in order to remove a small amount of aggregated proteins. Final preparations of the mutant enzymes were also chromatographed on a Sephadex G-100 column so as to replace the medium with 0.2 M NaCl.

The concentrations of all SMases were determined spectrophotometrically based on the molar absorption coefficient of 5.82×10^4 $M^{-1} \cdot cm^{-1}$ at 280 nm, which was calculated from the Tyr and Trp contents (*11*) and their respective molar absorption coefficients of 1.4×10^3 and 5.5×10^3 $M^{-1} \cdot cm^{-1}$ at 280 nm (*12*). The final enzyme solutions were stored at 4°C.

Measurements of Circular Dichroism (CD) and Fluorescence—CD spectra were measured in the far-ultraviolet region at 37°C and ionic strength 0.2, as previously described (*5*). The protein concentrations were 0.04-0.05 mg/ml. The mean residue ellipticity, $[\theta]$, was obtained from the equation: $[\theta] = (100 \times \theta)/(l \times c)$, where θ, l, and c are the observed ellipticity in degrees, the path length of the cell in centimeters, and the residue molar concentration of protein, respectively. An average residue molecular weight of 112 was used for calculating the residue molar concentration.

Tryptophyl fluorescence spectra were measured at 25°C and ionic strength 0.2 as previously described (*5*). Final concentration of protein was $1\text{-}2 \times 10^{-7}$ M.

Measurements of SMase Activity—Enzymatic hydrolysis of stereoisomers of monodispersed short-chain SM analogs was measured at 25°C, pH 7.0, and ionic strength 0.2 by the pH-stat assay method. The concentrations of the substrates and Mg^{2+} were 3 and 13 mM, respectively. Hydrolysis of micellar HNP was measured spectrophotometrically according to the method of Gal *et al.* (*13*) at 37°C and ionic strength 0.2, as described previously (*5*). Hydrolysis of micellar SM mixed with Triton X-100 (1:10) was measured at 25°C and ionic strength 0.2 by the pH-stat assay method, as described previously (*5*). At pH values below 7, the observed titration volumes are apparent, since the phosphate moiety of the released phosphocholine molecule does not completely dissociate in this pH range. The observed titration volumes were therefore corrected by using the degree of dissociation, α, of phosphocholine at a given pH value: $\alpha = 1/(1 + 10^{pK - pH})$ where the value of dissociation constant, pK, is 5.72 (*14*).

RESULTS

Conformational Stability of Mutant SMases—To test whether replacement of the amino acid residues resulted in gross structural changes of proteins, we measured the CD spectra of WT and mutant SMases at 37°C, pH 6.0, and ionic strength 0.2. All the enzymes exhibited similar spectra, indicating a lack of significant change in the secondary structure of the proteins (data not shown).

Previously, we revealed that WT SMase was structurally stable in the pH range from 5.0 to 9.0 (*5*). To examine the structural stability of mutant SMases, the negative ellipticities at 222 nm of WT and mutant SMases were measured at 37°C and pH 5.0, 6.0, and 8.5. As shown in Table I, the negative ellipticities of all the SMases were nearly identical to one another and no significant changes were observed within 30 min. Therefore, all the experiments described below were performed within the pH range from 5.0 to 8.5.

Hydrolysis of Short-Chain SM Analogs by Mutant SMases—We recently developed an efficient method for synthesis of short-chain SM analogs that can act as monodispersed substrates of SMases (*9*). Table II shows the hydrolytic activities of WT and mutant SMases toward several optical isomers of SM analogs (C_6C_{10}SPC and

TABLE I. **pH dependence of the negative ellipticities at 222 nm of WT and mutant SMases.** The negative ellipticities, $[\theta]$, at 222 nm of WT, D126G, and D156G SMases were measured in the presence of 1 mM EDTA at 37°C and ionic strength 0.2.

SMase	$[\theta] \times 10^{-3}$ at 222 nm					
	pH 5.0		pH 6.0		pH 8.5	
	0 min	30 min	0 min	30 min	0 min	30 min
WT[a]	−8.4	−8.3	−8.6	−8.6	−8.4	−8.5
D126G	−8.2	−8.2	−8.2	−8.1	−7.9	−7.7
D156G	−8.2	−8.3	−8.3	−8.3	−8.2	−7.9

[a]Data cited from Ref. *5*.

TABLE II. **Initial velocities of the hydrolysis of short-chain SM analogs catalyzed by WT and mutant SMases.** The enzyme activities were measured at 3 mM of substrate in the presence of 13 mM Mg^{2+} at 25°C, pH 7.0, and ionic strength 0.2.

Substrate	Activity (μmol/min/mg)		
	WT	D126G	D156G
Monodispersed C_6C_{10}SPC			
D-*erythro* form	136.31±15.92	66.95±5.52	226.46±8.16
L-*erythro* form	19.56±1.47	8.93±1.06	37.28±0.24
L-*threo* form	11.17±1.08	—	5.68±0.70
D-*threo* form	—	—	—
Monodispersed C_6C_{10}DSPC			
D-*erythro* form	109.15±2.04	39.90±2.87	269.26±9.72

Dashed lines: not detectable.

C_6C_{10}DSPC) in the presence of 13 mM Mg^{2+} at 25°C, pH 7.0, and ionic strength 0.2.

The initial velocities were measured in triplicate at an initial substrate concentration of 3 mM. Since the critical micellar concentration (cmc) of D-*erythro* C_6C_{10}SPC was more than 7 mM (data not shown), all of the short-chain SM analogs used were considered to be dispersed as monomers in solution under the present experimental conditions.

The WT SMase-catalyzed hydrolysis of D-*erythro* C_6C_{10}SPC, which is a naturally occurring isomer, was more rapid than that of other optical isomers of C_6C_{10}SPC. The enzymatic activities toward the L-*erythro* and L-*threo* forms of C_6C_{10}SPC were about 10-times lower than that toward the D-*erythro* form, and the activity toward the D-*threo* form was too low to be detected. On the other hand, the enzyme activity toward D-*erythro* C_6C_{10}DSPC, which is the dihydro-form of C_6C_{10}SPC, was comparable to that toward D-*erythro* C_6C_{10}SPC. This suggests that the double bond in SM is not essential for the enzymatic catalysis by *B. cereus* SMase.

The activity of WT SMase toward D-*erythro* C_6C_{10}SPC was about two times higher than that of D126G but about two times lower than that of D156G SMase. Similar tendencies were observed for two other substrates, L-*erythro* C_6C_{10}SPC and D-*erythro* C_6C_{10}DSPC.

Binding of Mg^{2+} to Mutant SMases—Since Mg^{2+} is prerequisite for the enzyme activity of *B. cereus* SMase, the binding of Mg^{2+} to the mutant enzymes was studied. The fluorescence maximum at 340 nm for both of the mutant SMases slightly decreased in intensity on addition of Mg^{2+}. Thus the decrease in the fluorescence intensity at 340 nm, $|\Delta F|$, and the initial velocity of micellar HNP hydrolysis at its saturating concentration, v, were plotted against logarithmic molar concentration of Mg^{2+}, log C_M (Fig. 1). In the Mg^{2+}-dependence curve of $|\Delta F|$ for each of the two mutants, two transitions were observed, suggesting the existence of at least two binding sites for Mg^{2+}, with high and low affinities, as was previously found for WT enzyme. Figure 1 also shows that the binding of Mg^{2+} to the low-affinity site of mutant SMases was essential for the catalysis, as was the case for WT enzyme (*5*).

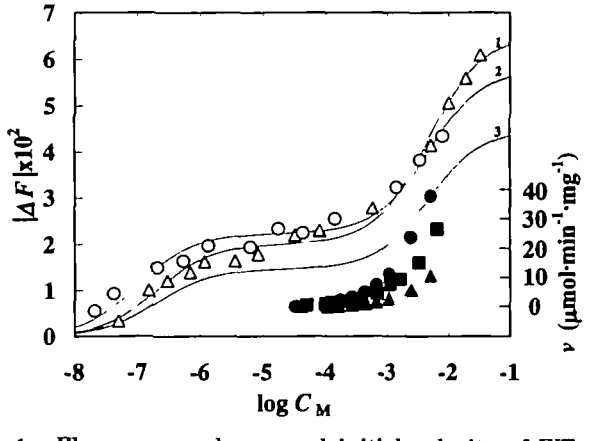

Fig. 1. **Fluorescence change and initial velocity of WT and mutant SMases on addition of Mg^{2+}.** The changes in the tryptophyl fluorescence at 340 nm, excited at 290 nm, $|\Delta F|$, of D126G (△) and D156G (▽) SMases on addition of Mg^{2+} at 25°C, pH 6.0, and ionic strength 0.2, plotted as a function of the logarithm of the total molar concentration of Mg^{2+}, C_M. Solid lines 1, 2, and 3 indicate the theoretical curves for D126G, D156G, and WT SMases, respectively, drawn according to Eq. 1 using the parameters indicated in the text. The initial velocities of the hydrolysis of micellar HNP at its saturating concentration, v, were determined for D126G (▲), D156G (●), and WT (■) SMases at 37°C, pH 6.0, and ionic strength 0.2. The initial velocity data for D126G plotted in this figure were magnified 20 times, since they were too small to be plotted exactly as they were. The data for WT enzyme were taken from Ref. *5*.

In the foregoing study, we determined the binding constants of Mg^{2+} to the low- and high-affinity sites of WT SMase, according to the following equation (*5*).

$$|\Delta F| = \frac{A \cdot C_M + B \cdot C_M^2}{1 + \frac{C_M}{K^{EM}} + \frac{C_M^2}{K^{EMM} \cdot K^{EM}}}, \quad (1)$$

where K^{EMM} and K^{EM} are the macroscopic dissociation constants of Mg^{2+} from the low- and high-affinity sites, respectively, and A and B are constants.

The data in Fig. 1 for both of the mutants were analyzed according to Eq. 1. The solid curves shown in Fig. 1 are the most probable theoretical ones, drawn by use of the parameters $1/K^{EMM} = 2.1\times10^2$ M^{-1}, $1/K^{EM} = 5.0\times10^6$ M^{-1}, $A = 1.0\times10^5$ M^{-1}, and $B = 6.8\times10^7$ M^{-2} for D126G, and $1/K^{EMM} = 2.1\times10^2$ M^{-1}, $1/K^{EM} = 1.0\times10^7$ M^{-1}, $A = 2.2\times10^5$ M^{-1}, and $B = 1.2\times10^8$ M^{-2} for D156G. Each set of binding constants of Mg^{2+} to the low- and high-affinity sites of the two mutant SMases was nearly identical to that of WT enzyme ($1/K^{EMM} = 2.1\times10^2$ M^{-1} and $1/K^{EM} = 5.0\times10^6$ M^{-1}) (*5*).

Effect of Mg^{2+} on the Enzymatic Hydrolysis of SM—Figure 2 shows the Lineweaver-Burk plots of the hydrolysis by D126G and D156G SMases of micellar SM mixed with Triton X-100 (1:10) at 25°C, pH 6.0, and ionic strength 0.2 at various concentrations of Mg^{2+} above that required to saturate the high-affinity binding site for Mg^{2+}. The values of apparent maximum velocity, V_{max}^{app}, and apparent Michaelis constant, K_m^{app}, were determined from the respective hyperbolic curves of velocity data by using non-linear regression analysis.

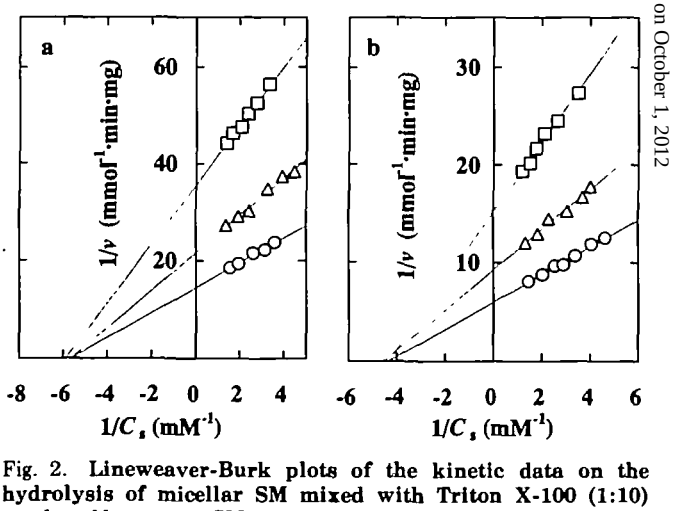

Fig. 2. **Lineweaver-Burk plots of the kinetic data on the hydrolysis of micellar SM mixed with Triton X-100 (1:10) catalyzed by mutant SMases.** The initial velocities of the hydrolysis of micellar SM mixed with Triton X-100 (1:10), catalyzed by D126G (a) and D156G (b) SMases, were measured in the presence of various molar concentrations of Mg^{2+} (▽, 13.3 mM; △, 6.65 mM; □, 3.33 mM) at 25°C, pH 6.0, and ionic strength 0.2.

For both of the mutants, V_{max}^{app} increased with increase in the Mg^{2+} concentration, whereas K_m^{app} remained unchanged. Similar results were obtained at pH 5.0 and 8.0 and also when micellar HNP was used as the substrate (data not shown).

The kinetic parameters K_m^{app}/V_{max}^{app} and $1/V_{max}^{app}$ for a given molar concentration of Mg^{2+}, C_M, are expressed by the following equations (*5*):

$$\frac{K_m^{app}}{V_{max}^{app}} = \frac{K_m \cdot K^{EMM}}{V_{max}} \cdot \frac{1}{C_M} + \frac{K_m}{V_{max}} \quad (2)$$

and

$$\frac{1}{V_{max}^{app}} = \frac{K^{EMSM}}{V_{max}} \cdot \frac{1}{C_M} + \frac{1}{V_{max}}, \quad (3)$$

where K_m and V_{max} are the Michaelis constant and maximum velocity when the enzyme is saturated with Mg^{2+} at both the high- and low-affinity binding sites. K^{EMM} and K^{EMSM} are the dissociation constants of Mg^{2+} from the low-affinity site of the enzyme-Mg^{2+} and the enzyme-substrate-Mg^{2+} complexes, respectively.

To determine the K^{EMM} and K^{EMSM} values, the values of K_m^{app}/V_{max}^{app} and $1/V_{max}^{app}$ in Fig. 2 for the two mutants were plotted against $1/C_M$, according to Eqs. 2 and 3, respectively (data not shown). The values of $1/K^{EMM}$ and $1/K^{EMSM}$ for D126G were determined to be $9.3 \pm 0.9 \times 10^1\ M^{-1}$ and $8.0 \pm 1.7 \times 10^1\ M^{-1}$, respectively, and those for D156G to be $6.7 \pm 0.5 \times 10^1\ M^{-1}$ and $7.6 \pm 0.6 \times 10^1\ M^{-1}$. All these values were comparable to each other, being consistent with the values ($1/K^{EMM}$) determined by fluorescence measurement (Fig. 1).

The experiments were repeated at pH 5.0 and 8.0 with the same substrate and at pH 5.0, 6.0, and 8.0 with micellar HNP as the substrate. At each pH value tested, the binding constants of Mg^{2+} to the low-affinity site were found to be very similar to each other, irrespective of the type of enzyme and substrate used and of the presence or absence of the substrate (data not shown).

pH-Dependence of the Binding Constant of Mg^{2+} to the Low-Affinity Site—When micellar HNP was used as the substrate at a concentration high enough to saturate the enzyme, the initial velocity, v, can be replaced by V_{max}^{app}. Thus, the binding constants of Mg^{2+} to the low affinity site, $1/K^{EMSM}$, could be easily determined according to Eq. 3 from the plots of the initial velocity *versus* the Mg^{2+} concentration. We determined the logarithm of Mg^{2+}-binding constant to the low-affinity site of WT and mutant SMases at various pH values at 37°C and ionic strength 0.2 (Fig. 3). The binding constants of Mg^{2+} to the low-affinity sites of the three enzymes proved to be nearly identical to each other at each pH value.

pH-Dependence of the Kinetic Parameters for the Hydrolysis of Micellar SM Mixed with Triton X-100 and Micellar HNP—Figure 4a shows the pH-dependence of the log ($1/K_m$) of WT, D126G, and D156G enzymes for the hydrolysis of micellar SM mixed with Triton X-100 (1:10) at 25°C and ionic strength 0.2, at Mg^{2+} concentrations sufficient to saturate both the low- and high-affinity binding sites. Figure 4b shows comparable data for the hydrolysis of micellar HNP at 37°C. The values of K_m could be replaced directly by the K_m^{app} values at appropriate concentrations of Mg^{2+}, which were determined using non-linear regression analysis from the respective hyperbolic curves of velocity *versus* substrate concentration, since the binding of substrate was independent of Mg^{2+} binding to the

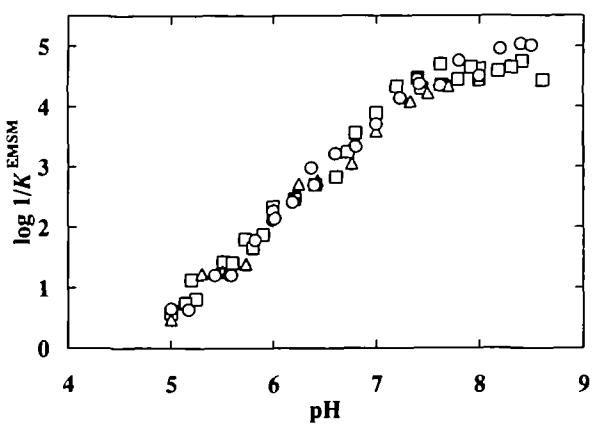

Fig. 3. **pH-dependence of the logarithm of the binding constant of Mg^{2+} to the low-affinity site of WT and mutant SMases.** The binding constants of Mg^{2+} to the low affinity site of D126G (∠), D156G (◡), and WT ( ) SMases were measured in the presence of HNP concentrations high enough to saturate the binding site at 37°C and ionic strength 0.2. The data for WT enzyme were taken from Ref. *5*.

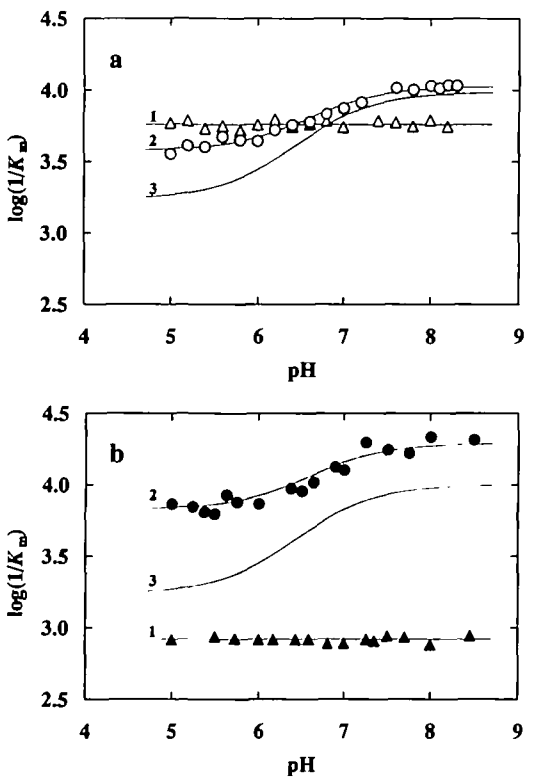

Fig. 4. **pH-dependence of the logarithm of $1/K_m$ of WT and mutant SMases.** The $1/K_m$ values of D126G (triangles) and D156G (circles) SMases for the hydrolysis of micellar SM mixed with Triton X-100 (1:10) (a) and micellar HNP (b), were measured in the presence of Mg^{2+} concentrations high enough to saturate both the high- and low-affinity binding sites at ionic strength 0.2. Solid lines 1, 2, and 3 indicate the theoretical curves for D126G, D156G, and WT SMases, respectively, drawn according to Eq. 4 using the parameters indicated in the text. The data for WT enzyme were taken from Ref. *5*.

enzyme, as described above (Fig. 2). The pH-dependence curve of D156G for each of the two substrates showed a single transition between pH 6 and 7, indicating the participation of one ionizable group. On the other hand, no significant transitions were observed in the corresponding curves for D126G.

When a single ionizable group participates in the substrate binding, the logarithm of $1/K_m$ obtained at a given pH value may be expressed by the following equation, as previously described (*5*).

$$\log\frac{1}{K_m}=\log\frac{\frac{[H^+]}{K^{EM_2SH}}+1}{\frac{[H^+]}{K^{EM_2H}}+1}+\log\frac{1}{k_m}, \quad (4)$$

where K^{EM_2H} and K^{EM_2SH} are the dissociation constants of protons from the enzyme-Mg^{2+} and enzyme-Mg^{2+}-substrate complexes, respectively. The term $1/k_m$ is the limiting value of $1/K_m$ when the ionizable group in question is completely deprotonated.

The solid curves for D156G SMase in Fig. 4 are the most probable theoretical ones, drawn according to Eq. 4 using the parameters $pK^{EM_2SH}=6.36$, $pK^{EM_2H}=6.81$, and $1/k_m=1.07\times10^4\ M^{-1}$ for micellar SM mixed with Triton X-100, and the parameters $pK^{EM_2SH}=6.35$, $pK^{EM_2H}=6.81$, and $1/k_m=1.95\times10^4\ M^{-1}$ for micellar HNP. In the case of D126G, the values of $1/K_m$ were independent of pH irrespective of the substrate, and the straight lines are drawn using the $1/K_m$ values of $5.75\times10^3\ M^{-1}$ and $8.32\times10^2\ M^{-1}$, for micellar SM mixed with Triton X-100 and micellar HNP, respectively.

Figure 5a shows the pH-dependence of log k_{cat} of WT and mutant SMases for the hydrolysis of micellar SM mixed with Triton X-100 (1:10) at 25°C and ionic strength 0.2, in the presence of essentially saturating concentration of Mg^{2+}. Similar analysis for micellar HNP hydrolysis at 37°C is also expressed in Fig. 5b. The k_{cat}^{app} values at appropriate concentrations of Mg^{2+}, which were determined from the respective hyperbolic curves of velocity *versus* substrate concentration using non-linear regression analysis, were replaced by the values of k_{cat}, corrected for the complete Mg^{2+} complexes by using the dissociation constants for Mg^{2+} of K^{EMSM} ($=K^{EMM}$), which were obtained from Fig. 3 according to Eq. 3.

The pH-dependence curve of k_{cat} for D126G SMase with each of the substrates showed two transitions, one below pH 6 and one above pH 7.5, indicating the participation of two ionizable groups. These two transitions appeared to have slopes of +1 and −1, respectively, suggesting that deprotonation of an acidic ionizable group and protonation of a basic ionizable group are essential for the catalysis.

Regarding the ionization states of the two ionizable groups in question, there are four microscopic forms of enzyme-substrate-Mg^{2+} complex. Only one of these species, the complex having deprotonated acidic and protonated basic ionizable groups, was assumed to produce the product with a rate constant of $k_{cat,1}$. The logarithm of k_{cat} at a given pH value may be expressed by the following equation (*5*).

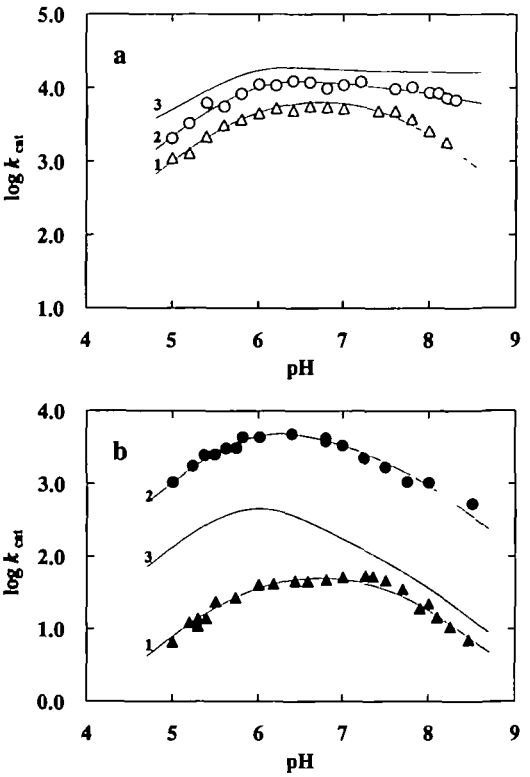

Fig. 5. **pH-dependence of the logarithm of k_{cat} of WT and mutant SMases.** The k_{cat} values of D126G (triangles) and D156G (circles) SMases for the hydrolysis of micellar SM mixed with Triton X-100 (1:10) (a) and micellar HNP (b), were measured in the presence of Mg^{2+} concentrations high enough to saturate both the high- and low-affinity binding sites at ionic strength 0.2. Solid lines 1, 2, and 3 indicate the theoretical curves for D126G, D156G, and WT SMases, respectively, drawn according to Eqs. 5 or 6 using the parameters indicated in the text. The data for WT enzyme were taken from Ref. *5*.

$$\log k_{cat}=\log\frac{D\cdot[H^+]}{\frac{[H^+]^2}{K^{EM_2SH_2}\cdot K^{EM_2SH_1}}+\frac{[H^+]}{K^{EM_2SH_1}}+1}, \quad (5)$$

where $K^{EM_2SH_2}$ and $K^{EM_2SH_1}$ are the macroscopic dissociation constants of protons from the two ionizable groups in question of the enzyme-Mg^{2+}-substrate complex. D is the constant expressed by

$$D=\frac{k_{cat,1}}{k_1^{EM_2SH_1}}, \quad (6)$$

where $k_1^{EM_2SH_1}$ is the microscopic dissociation constant of the microscopic form of enzyme-substrate-Mg^{2+} complex having the deprotonated acidic and protonated basic ionizable groups into a proton and the microscopic form of the complex having the deprotonated acidic and basic ionizable groups (*5*).

The solid curves for D126G SMase shown in Fig. 5 are the most probable theoretical ones, drawn according to Eq. 5 using the parameters of $pK^{EM_2SH_2}=5.85$, $pK^{EM_2SH_1}=7.60$, and $D=3.23\times10^{11}\ M^{-1}\cdot min^{-1}$ for micellar SM mixed with Triton X-100, and of $pK^{EM_2SH_2}=5.85$, $pK^{EM_2SH_1}=7.60$, and $D=2.54\times10^9\ M^{-1}\cdot min^{-1}$ for micellar HNP.

As shown in Fig. 5, the pH-dependence curves of k_{cat} for D156G SMase with the two substrates were similar in

shape to those for WT enzyme. Previously, the pH-dependence of k_{cat} of WT SMase for the hydrolysis of micellar SM mixed with Triton X-100 and of micellar HNP was analyzed on the assumption that three ionizable groups participate in the catalytic activity and that deprotonation of the most acidic group is essential for the catalysis, according to the following equation (*5*).

$$\log k_{cat} = \log \frac{A \cdot [H^+]^2 + B \cdot [H^+] + C}{\frac{[H^+]^3}{K^{EM_2SH_3} \cdot K^{EM_2SH_2} \cdot K^{EM_2SH_1}} + \frac{[H^+]^2}{K^{EM_2SH_2} \cdot K^{EM_2SH_1}} + \frac{[H^+]}{K^{EM_2SH_1}} + 1} \quad (7)$$

where $K^{EM_2SH_3}$, $K^{EM_2SH_2}$, and $K^{EM_2SH_1}$ are the macroscopic dissociation constants of protons from the three ionizable groups of the enzyme-Mg^{2+}-substrate complex, and A, B, and C are the constants as previously described (*5*).

The data for D156G were analyzed in the same way as those for WT enzyme. As the pK values of the second ionizable group of the enzyme-Mg^{2+}-substrate complexes, we used the values of $pK^{EM_2SH_2} = 6.36$ for SM and 6.35 for HNP, which were determined from the pH-dependence data of $1/K_m$. As the pK values of the first and third ionizable groups for D156G SMase, we used the values of $pK^{EM_2SH_3} = 5.85$ and $pK^{EM_2SH_1} = 7.60$, for both of the substrates. Other parameters thus determined according to Eq. 7 were $A = 6.30 \times 10^{18}$ $M^{-2} \cdot min^{-1}$, $B = 1.68 \times 10^{12}$ $M^{-1} \cdot min^{-1}$, and $C = 4.44 \times 10^3$ min^{-1} for SM and $A = 7.47 \times 10^{17}$ $M^{-2} \cdot min^{-1}$ and $B = 1.25 \times 10^{11}$ $M^{-1} \cdot min^{-1}$ for HNP. In the case of HNP, the protonation of the most basic group was essential for the catalysis, and the constant C in Eq. 7 was therefore neglected as described previously (*5*).

The solid curves in Fig. 5 are the most probable theoretical ones, and they agreed well with the pH-dependence data for both of the enzymes as well as both of the substrates.

DISCUSSION

Hydrolysis of Short-Chain SM Analogs by Mutant SMases—Lipid-hydrolyzing enzymes such as phospholipase A_2 generally react with micellar or aggregated substrates at much greater rates than with monodispersed substrates (*16*). This is thought to be due to the additional substrate binding to the interfacial recognition site, which is distinct from the catalytic site of the enzyme molecule (*17*). Therefore, studies of the hydrolysis of monodispersed substrates are very useful to elucidate the catalytic mechanism of these kinds of enzymes, since the participation of the interfacial recognition site can be excluded.

As can be seen from Table II, the hydrolysis of monodispersed D-*erythro* C_6C_{10}SPC by WT enzyme was more efficient than those of other isomers, and the double bond in the substrate molecule had no significant effect on the hydrolysis. Previously, Barnholz *et al.* (*18*) studied the hydrolysis of two isomers of micellar *N*-palmitoyl-SPC and *N*-palmitoyl-DSPC mixed with Triton X-100, using partially purified SMase from rat brain. Their results suggested that the hydrolysis of SM in the D-*erythro* form was five times faster than that in the L-*erythro* form and that the double bond in SM had no significant effect on the hydrolysis. These findings are compatible with our present results. Thus we concluded that the configuration of SM is not critical in interfacial recognition but very important in catalytic activity.

As can also be seen from Table II, there were no differences in stereosensitivity between WT and mutant SMases. This result suggested that Asp126 and Asp156 had no significant effects on the stereospecificity.

Previously, we compared the hydrolytic activities of D126G and D156G SMases with that of WT enzyme toward four kinds of substrates having different hydrophobicities, SM, HNP, lysophosphatidylcholine (lyso-PC), and *p*-nitrophenylphosphocholine (*p*-NPPC) (*6, 7*). D126G exhibited weaker activity toward all of the substrates than did the WT enzyme, whereas D156G hydrolyzed the water-soluble substrates containing a *p*-nitrophenyl group (HNP and *p*-NPPC) more effectively than the WT enzyme. Under the experimental conditions, HNP and *p*-NPPC were thought to exist in micellar and monodispersed states, respectively. Therefore, the high activity of D156G toward HNP and *p*-NPPC seemed to be due to the hydrophylicity or *p*-nitrophenyl group of these substrates. In the present study, similar high activity of D156G was observed toward monodispersed short-chain SM analogs (Table II). Therefore, the high activity exhibited by D156G can be ascribed to the hydrophylicity of the substrates used, rather than to the presence of a *p*-nitrophenyl group or to the micellar or monodispersed states of the substrates.

Effect of Replacement of Asp126 or Asp156 with Gly on the Mg^{2+} Binding—Recently, we showed that WT SMase has at least two binding sites for Mg^{2+}, and that the binding to the low-affinity site was essential for the catalysis but independent of the substrate binding to the enzyme (*5*). As shown in Figs. 1 and 2, similar results were obtained for D126G and D156G SMases. Moreover, the binding constants of Mg^{2+} to the low-affinity sites of WT, D126G, and D156G SMases were nearly identical to each other at several pH values (Fig. 3). These results indicate that Asp126 and Asp156 do not participate in the Mg^{2+} binding to the enzyme.

Roles of Asp126 and Asp156 in the Enzyme Activity toward Micellar Substrates—Figure 4 shows that the pH-dependence curves of $1/K_m$ for D156G SMase toward the two substrates, SM and HNP, were of similar shape and revealed a single transition. Similar results were obtained for WT enzyme (*5*). These results indicate that an ionizable group with a pK value of 6.81 participated in the substrate binding, and its pK values were lowered upon binding of HNP and SM, suggesting that deprotonation of this ionizable group enhanced the binding of both substrates. On the other hand, D126G SMase showed no transitions in the pH-dependence curve of $1/K_m$ for either substrate. On the basis of this observation, the ionizable group which participates in the substrate binding to *B. cereus* SMase was assigned to Asp126, although its pK value was anomalously high, and the ionization of this residue was found to enhance the substrate binding about fivefold.

High pK values of Asp residues have been reported for other enzymes. *Escherichia coli* thioredoxin Asp26, which is completely buried in a hydrophobic groove, has a pK value of 7.5 in the oxidized form of protein. Furthermore, in the presence of anionic Cys32 (the reduced form), the pK value of Asp26 is 9.2 (*19*). A pK of 8.5 has also been reported for Asp99 in 3-oxo-Δ^5-steroid isomerase, in which the side chain of this amino acid residue is found in an extremely hydrophobic environment and there is an elec-

trostatic effect of negatively charged Asp38 in the proximity of Asp99 (*20*). In addition, the Asp residue in a synthetic protein-based polymer was shown to have a pK value of 10 in the hydrophobic environment created by five proximal Phe residues (*21*). On the basis of these observations, it is thought that Asp126 in *B. cereus* SMase is located in a hydrophobic environment and/or very close to negatively charged amino acid residues.

With regard to the $1/K_m$ values at acidic pH, where the negative charge at position 126 is abolished by protonation, these values were unexpectedly increased by the replacement of Asp126 or Asp156 with Gly, except in the case of D126G acting on HNP. This suggests that Asp156 of WT SMase acts to decrease the binding of both substrates, while Asp126 also acts to decrease the binding of SM but not of HNP.

In Fig. 5, the pH-dependence curves of k_{cat} for D126G SMase toward both substrates showed two transitions, one below pH 6 and one above pH 7.5, having tangent lines with slopes of +1 and −1, respectively. On the other hand, the curve for D156G SMase toward HNP showed three distinct transitions: one below pH 6, one between pH 6.5 and 7, and one above pH 7.5. The first and third transitions had tangent lines with slopes of +1 and −1, respectively. The curve for D156G SMase toward SM showed one large transition below pH 6 having a tangent line with a slope of +1, and no large transitions were clearly observed in the alkaline pH region. Similar results were obtained with the WT enzyme.

pH-dependence data on k_{cat} were analyzed on the basis of the following three assumptions. (i) The ionizable groups of three amino acids fundamentally participate in the catalytic activity of SMase, since it could be postulated that the basic catalytic mechanism of the enzyme is independent of the substrate used. (ii) One amino acid among them having the pK value of 6.0-6.5 is Asp126, and its pK value was determined from pH-dependence curves of $1/K_m$. Therefore, the ionizable groups of only two amino acids participate in the catalytic activity of D126G SMase. (iii) The respective pK values of the other two amino acids were practically the same irrespective of the substrate and enzyme used.

Table III summarizes the pK values, which agreed well with the pH-dependence data for $1/K_m$ and k_{cat}, in accordance with the idea described above.

Matsuo *et al.* (*8*) suggested general-acid-base catalysis as the catalytic mechanism of *B. cereus* SMase, and that His296 and His151 work as a general base and acid, respectively, on the basis of the predicted three-dimensional structure and the results of site-directed mutagenesis studies. In the present study, pH-dependence curves of the logarithm of k_{cat} were shown to have a tangent line with the slope of +1 in the acidic pH range. The pK value of the ionizable group participating in this transition was determined to be 5.85, and this ionizable group was assigned to His296, which acts as a general base. The transition in the alkaline pH range, which involved an ionizable group having pK = 7.6 and had a tangent line with a slope of −1, was not observed for the case of SM hydrolysis catalyzed by WT and D156G SMases. Since this ionizable residue was very critical in the catalytic activity toward HNP but not toward SM, it could not be the catalytic residue. However, it is not clear why this ionizable group became so important in the catalysis toward SM when Asp126 was converted to Gly.

TABLE III. **Comparison of the pK values of ionizable groups participating in the substrate binding and catalytic activity of WT and mutant SMases.** The pK values were determined according to Eqs. 4-6 using the parameters indicated in the text.

Substrate	SMases	log $(1/K_m)$		log k_{cat}		
		pK^{EM_2SH}	pK^{EM_2H}	$pK^{EM_2SH_2}$	pK^{EM_2SH}	$pK^{EM_2SH_3}$
SM	WT[a]	6.06	6.81	5.85	6.06	7.60
	D126G	—	—	5.85	—	7.60
	D156G	6.36	6.81	5.85	6.36	7.60
HNP	WT[a]	6.05	6.81	5.85	6.05	7.60
	D126G	—	—	5.85	—	7.60
	D156G	6.35	6.81	5.85	6.35	7.60
Putative residues		Asp126		His296[b]	Asp126	?

Dashed lines: not determined. [a]Data cited from Ref. *5*. [b]Cited from Refs. *5* and *8*.

As shown in Fig. 5, the k_{cat} values of the mutant SMases were smaller than that of WT at all pH values, except in the case of D156G hydrolysis of HNP. It was suggested that Asp126 of WT SMase acts to enhance the catalytic activity toward both substrates, and Asp156 also acts to enhance the catalytic activity toward SM but not toward HNP. From the pH-dependence curve of the WT enzyme, the ionization of Asp126 was found to slightly decrease the catalytic activity.

As described above, the values of kinetic parameters of WT and two mutants (D126G and D156G) were different from each other, even if the experiments were performed at acidic pH. This result can not be interpreted in terms of the ionization of Asp residues, since the negative charge of at least one of the Asp residues at position 126 and 156 should no longer contribute under that condition. If we had used other kinds of mutants having these residues substituted by residues such as Asn or Ala instead of Gly, such a large discrepancy might not have been observed. Nevertheless, the fact that the values of kinetic parameters were changed by the replacement of Asp with Gly implies that these two Asp residues participate in the substrate binding and catalytic activity of SMase.

The predicted three-dimensional structure of *B. cereus* SMase suggests that these two Asp residues are located close to the active site (*8*) and to the disulfide bond Cys123-Cys156 (*15*). As can be seen from Table I, no significant changes in the negative ellipticity at 222 nm were observed in the mutant enzymes. In the present study, we showed that the deprotonation of Asp126 enhances the substrate binding and slightly suppresses the catalytic activity, and consequently Asp126 was thought to be located close to the active site. We consider that the changes in the values of kinetic parameters by the replacement of Asp with Gly resulted from microscopic conformational changes at the active site of the enzyme.

REFERENCES

1. Tomita, M., Taguchi, R., and Ikezawa, H. (1991) Sphingomyelinase of *Bacillus cereus* as a bacterial hemolysin. *J. Toxicol. Toxin Rev.* **10**, 169-207
2. Hannun, Y.A. (1994) The sphingomyelin cycle and the second messenger function of ceramide. *J. Biol. Chem.* **269**, 3125-3128
3. Liu, B., Obeid, L.M., and Hannun, Y.A. (1997) Sphingomyelinases in cell regulation. *Semin. Cell Dev. Biol.* **8**, 311-322
4. Tomiuk, S., Hofmann, K., Nix, M., Zumbansen, M., and Stoffel,

W. (1998) Cloned mammalian neutral sphingomyelinase: functions in sphingolipid signaling? *Proc. Natl. Acad. Sci. USA* **95**, 3638-3643
5. Fujii, S., Inoue, B., Yamamoto, H., Ogata, K., Shinki, T., Inoue, S., Tomita, M., Tamura, H., Tsukamoto, K., Ikezawa, H., and Ikeda, K. (1998) Mg^{2+} binding and catalytic function of sphingomyelinase from *Bacillus cereus*. *J. Biochem.* **124**, 1178-1187
6. Tamura, H., Tameishi, K., Yamada, A., Tomita, M., Matsuo, Y., Nishikawa, K., and Ikezawa, H. (1995) Mutation in aspartic acid residues modifies catalytic and haemolytic activities of *Bacillus cereus* sphingomyelinase. *Biochem. J.* **309**, 757-764
7. Ikezawa, H., Tameishi, K., Yamada, A., Tamura, H., Tsukamoto, K., Matsuo, Y., and Nishikawa, K. (1995) Studies on the active sites of *Bacillus cereus* sphingomyelinase substitution of some amino acids by site-directed mutagenesis. *Amino Acids* **9**, 293-298
8. Matsuo, Y., Yamada, A., Tsukamoto, K., Tamura, H., Ikezawa, H., Nakamura, H., and Nishikawa, K. (1996) A distant evolutionary relationship between bacterial sphingomyelinase and mammalian DNase I. *Protein Sci.* **5**, 2459-2467
9. Murakami, M., Iwama, S., Fujii, S., Ikeda, K., and Katsumura, S. (1997) An efficient synthesis of short-chain sphingomyelin analogs and their susceptibility to hydrolysis catalyzed by sphingomyelinase. *Bioorg. Med. Chem. Lett.* **7**, 1725-1728
10. Fiske, C.H. and Subbarow, Y. (1925) The colorimetric determination of phosphorus. *J. Biol. Chem.* **66**, 375-400
11. Yamada, A., Tsukagoshi, N., Udaka, S., Sasaki, T., Makino, S., Nakamura, S., Little, C., Tomita, M., and Ikezawa, H. (1988) Nucleotide sequence and expression in *Escherichia coli* of the gene coding for sphingomyelinase of *Bacillus cereus*. *Eur. J. Biochem.* **175**, 213-220
12. Wetlaufer, D.B. (1962) Ultraviolet spectra of proteins and amino acids in *Advances in Protein Chemistry* (Anfinsen, C.B., Jr., Anson, M.L., Bailey, K., and Edsall, J.T., eds.) Vol. 17, pp. 303-390, Academic Press, New York
13. Gal, A.E., Brady, R.O., Hibbert, S.R., and Pentchev, P.G. (1975) Practical chromogenic procedure for the detection of homozygotes and heterozygous carriers of Niemann-Pick disease. *N. Engl. J. Med* **293**, 632-636
14. Ikeda, K., Inoue, S., Amasaki, C., Teshima, K., and Ikezawa, H. (1991) Kinetics of the hydrolysis of monodispersed and micellar phosphatidylcholines catalyzed by a phospholipase C from *Bacillus cereus*. *J. Biochem.* **110**, 88-95
15. Tomita, M., Ueda, Y., Tamura, H., Taguchi, R., and Ikezawa, H. (1993) The role of acidic amino-acid residues in catalytic and adsorptive sites of *Bacillus cereus* sphingomyelinase. *Biochim. Biophys. Acta* **1203**, 85-92
16. Fujii, S., Inoue, T., Inoue, S., and Ikeda, K. (1991) Kinetics of the hydrolysis of monodispersed dihexanoylphosphatidylcholine catalyzed by bovine pancreatic phospholipase A_2: Roles of Ca^{2+} binding and ionizations of amino acid residues in the active site. *J. Biochem.* **110**, 1008-1015
17. Scott, D.L. and Sigler, P.B. (1994) Structure and catalytic mechanism of secretory phospholipases A_2. *Adv. Protein Chem.* **45**, 53-88
18. Barnholz, Y., Roitman, A., and Gatt, S. (1966) Enzymatic hydrolysis of sphingolipids. II. Hydrolysis of sphingomyelin by an enzyme from rat brain. *J. Biol. Chem.* **241**, 3731-3737
19. Chivers, P.T., Prehoda, K.E., Volkman, B.F., Kim, B.-M., Markley, J.L., and Raines, R.T. (1997) Microscopic pK_a values of *Escherichia coli* thioredoxin. *Biochemistry* **36**, 14985-14991
20. Thornburg, L.D., Henot, F., Bash, D.P., Hawkinson, D.C., Bartel, S.D., and Pollack, R.M. (1998) Electrophilic assistance by Asp-99 of 3-oxo-Δ^5-steroid isomerase. *Biochemistry* **37**, 10499-10506
21. Urry, D.W., Gowda, D.C., Peng, S., Parker, T.M., Jing, N., and Harris, R.D. (1994) Nanometric design of extraordinary hydrophobic-induced pK_a shifts for aspartic acid: Relevance to protein mechanisms. *Biopolymers* **34**, 889-896